

## A baseball-bat-like CdTe/TiO<sub>2</sub> nanorods-based heterojunction core–shell solar cell

H. Karaagac,<sup>a,b,\*</sup> M. Parlak,<sup>b</sup> L.E. Aygun,<sup>c</sup> M. Ghaffari,<sup>c</sup> N. Biyikli<sup>a</sup>  
and A.K. Okyay<sup>a,c,\*</sup>

<sup>a</sup>UNAM-Institute of Materials Science and Nanotechnology, Bilkent University, Ankara 06800, Turkey

<sup>b</sup>Middle East Technical University, Department of Physics, Ankara 06800, Turkey

<sup>c</sup>Department of Electrical and Electronics Engineering, Bilkent University, Ankara 06800, Turkey

Received 2 April 2013; accepted 10 May 2013

Available online 18 May 2013

Rutile TiO<sub>2</sub> nanorods on fluorine-doped thin oxide glass substrates via the hydrothermal technique were synthesized and decorated with a sputtered CdTe layer to fabricate a core–shell type n-TiO<sub>2</sub>/p-CdTe solar cell. Absorbance spectrum verified the absorption contribution of both TiO<sub>2</sub> and CdTe to the absorption process. The solar cell parameters, such as open circuit voltage, short circuit current density, fill factor and power conversion efficiency were found to be 0.34 V, 1.27 mA cm<sup>-2</sup>, 28% and 0.12%, respectively.

© 2013 Acta Materialia Inc. Published by Elsevier Ltd. All rights reserved.

**Keywords:** Solar cell; Nanorod; Thin film

In recent years, TiO<sub>2</sub> (titanium dioxide) structures have attracted much attention because of their potential applications in various areas, such as solar cells [1], photo-electrochemical hydrogen production [2], field emission devices [3] and gas detectors [4]. However, TiO<sub>2</sub> nanorod (NR) based solar cells have become particularly interesting for enabling the production of highly efficient solar cells in a cost-effective way. Various solar cell device structures have been proposed based on vertically oriented NR, axial, core–shell (or radial) and NR embedded in thin films [5]. Of these device architectures, the core–shell, consisting of a one-dimensional (1-D) core semiconductor decorated with a thin layer (shell) of complementary material, is of particular interest to form a p–n heterojunction functioning as a solar cell in a radial direction. With such a device structure model, it is expected that the competition between light absorption and charge collection that exists in planar photovoltaic (PV) designs would be relieved by orthogonalization of these two processes and the possibility of separately optimizing light absorption and charge col-

lection. A core–shell solar cell offers not only enhanced light absorption (light trapping by NR), but also efficient charge collection (by single crystal channels of NR) to electrodes as long as core radius and shell thickness are optimized properly.

So far, numerous core–shell structures, including ZnO/Er<sub>2</sub>O<sub>3</sub>, ZnO/ZnS, V<sub>2</sub>O<sub>5</sub>/ZnO, ZnSe/CdS, ZnO/CdTe, TiO<sub>2</sub>/CdTe and CdS/CdTe, have been reported [6]. In addition, although there are numerous studies on dye-sensitized 1-D nanostructured solar cells, little effort has been focused on the integration of 1-D nanostructured inorganic materials to fabricate semiconductor-synthesized solar cells. Among type-II core–shell structures, TiO<sub>2</sub>/CdTe is a promising material combination because of the superior properties of TiO<sub>2</sub> NR and the excellent properties of the CdTe material pair, with an ideal band gap (1.45 eV) matching the most abundant part of the solar spectrum, a high absorption coefficient (10 × 10<sup>5</sup> cm<sup>-1</sup> at 700 nm) and long-term stability [7].

It is well known that there are three different polymorphs of TiO<sub>2</sub> (brookite, anatase and rutile), with different electrical and optical properties. Of these structures, the rutile phase is the most stable, which makes it a promising structure for nanomaterial-based opto-electronic applications [8]. As TiO<sub>2</sub> is a wide band

\* Corresponding authors. Address: UNAM-Institute of Materials Science and Nanotechnology, Bilkent University, Ankara 06800, Turkey. Tel.: +90 5377275121; e-mail addresses: [karaagac@unam.bilkent.edu.tr](mailto:karaagac@unam.bilkent.edu.tr); [aokyay@stanfordalumni.org](mailto:aokyay@stanfordalumni.org)

gap material ( $\sim 3.0$  eV for rutile  $\text{TiO}_2$  structure), it is unable to absorb sunlight in the visible range. However, a core-shell solar cell based on  $\text{TiO}_2/\text{CdTe}$  is expected to be suitable for the absorption of sunlight in a broad photon wavelength range, which plays a crucial role in the fabrication of high-efficiency low-cost solar cells.

A number of techniques have been reported for the synthesis of 1-D  $\text{TiO}_2$  nanostructures (NR, nanowires and nanotubes), including hydrothermal [9], electrochemical anodic oxidation [10] and chemical vapor deposition [11]. Among these, the hydrothermal technique offers several advantages over the others, owing to its simplicity, reaction velocity and cost suitability, which enables the construction of highly efficient solar cells on various substrates, such as glass [12], titanium [13] and fluorine-doped thin oxide (FTO) [14].

This paper reports an n- $\text{TiO}_2$ /p-CdTe core-shell solar cell constructed by a two-step route combining the hydrothermal method for the synthesis of  $\text{TiO}_2$  NR and the sputtering technique for the decoration of  $\text{TiO}_2$  NR with a thin CdTe layer. In other words, rutile  $\text{TiO}_2$  NR on FTO glass substrates via the hydrothermal technique were synthesized and subsequently decorated with a sputtered CdTe layer to fabricate a core-shell solar cell, the structural, electrical and optical properties of which were investigated in detail.

$\text{TiO}_2$  NR were synthesized on FTO ( $10 \times 50$  mm) substrate using hydrothermal growth technique, details of which have been given elsewhere [15,16]. The vertically well-oriented dense arrays of  $\text{TiO}_2$  NR obtained were coated with a  $\sim 250$ -nm-thick CdTe layer using the sputtering technique to form the n- $\text{TiO}_2$ /p-CdTe core-shell type solar cell. The deposition of the CdTe layer was carried out under  $1 \times 10^{-3}$  Torr Ar gas pressure at a  $\sim 0.6 \text{ \AA s}^{-1}$  deposition rate, employing 70 W RF power using a CdTe target, the thickness of which was monitored simultaneously by a quartz crystal monitor (Inficon XTM/2). Following the deposition of the CdTe layer, 10 nm Cu and 40 nm Au metallic layers of top contacts were deposited by thermal evaporation, using a dot-patterned copper shadow mask, and subsequently post-annealed at  $120^\circ\text{C}$  for 30 min to facilitate the formation of ohmic-type contacts. Structural characterization of the grown  $\text{TiO}_2$  NR and deposited CdTe thin film was carried out by performing X-ray diffraction (XRD) and transmission electron microscopy (TEM) measurements, using a Rigaku Miniflex model XRD system with a Cu  $K_\alpha$  X-ray source and an FEI Tecnai G2 F30 model, respectively. Surface morphology and cross-sectional images of  $\text{TiO}_2$  NR and solar cell structure were recorded using a FEI Nova Nanosem 430 model SEM microscope. A Varian Cary 5000 model UV-VIS-NIR spectrophotometer was used for the absorption measurement in the 350–1000 nm wavelength range. The photoresponsivity of the fabricated device was measured at a reverse bias of 0.5 V in the 300–900 nm wavelength range using a white light source, details of which are given elsewhere [15]. The solar cell performance of the fabricated device was tested in a Oriol 1000 W solar cell simulator setup (under AM 1.5 conditions).

Figure 1a and b shows the top view SEM images of  $\text{TiO}_2$  NR grown on a FTO pre-coated glass substrate re-

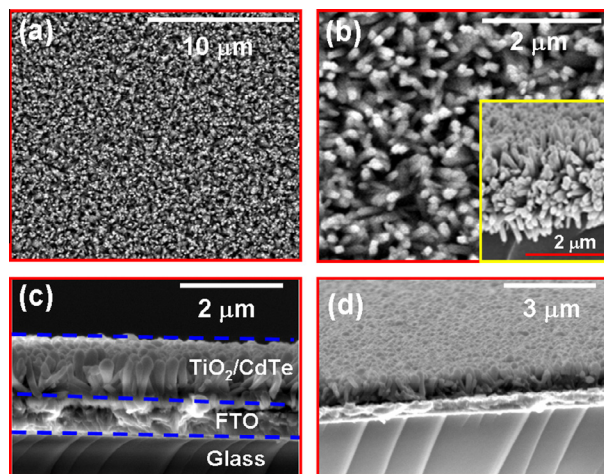


**Figure 1.** SEM images of  $\text{TiO}_2$  NR synthesized on a FTO pre-coated glass substrate recorded at (a) low magnification and (b) high magnification. (c) Cross-sectional and (d) tilted view of SEM images of  $\text{TiO}_2/\text{CdTe}$  core-shell solar cell.

corded at low-magnification and high-magnification, respectively. Figure 1a shows dense arrays of  $\text{TiO}_2$  NR, grown successfully and distributed homogeneously over the FTO surface. Figure 1b shows that the length of the synthesized NR is  $\sim 1.8 \mu\text{m}$ , and the average diameter is  $\sim 100$  nm. In Figure 1c and d, a SEM cross-sectional view and a tilted view of SEM micrographs of the constructed  $\text{TiO}_2/\text{CdTe}$  core-shell are indicated after decorating  $\text{TiO}_2$  NR with a sputtered  $\sim 250$ -nm-thick CdTe thin film. It is clear from these SEM images that the shape of  $\text{TiO}_2$  NR following the deposition of CdTe is baseball-bat-like. In other words, the diameter of the core-shell  $\text{TiO}_2$  increases from bottom to top.

In order to study the microstructure and morphology of the core-shell formed, TEM measurement was performed. Figure 2a shows a low-magnification TEM image of  $\text{TiO}_2$  NR coated with a CdTe thin film. The variation in diameter of the core-shell was also observed from TEM images, shown in Figure 2a and b. The formation of this type of core-shell can be attributed to the deposition parameters of CdTe. The deposition rate is playing a particularly important role in determining the form of core-shell, as a balanced crystal growth rate and deposition rate is required for a conformal coating of 1-D nanostructures. As reported earlier [6], when

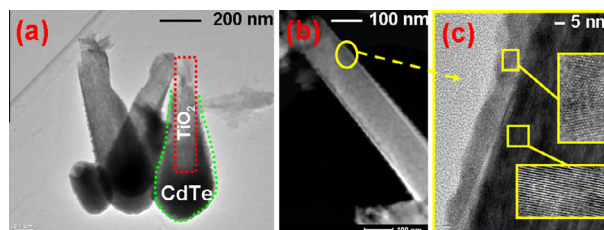


**Figure 2.** TEM images of CdTe decorated  $\text{TiO}_2$  NR: (a) low-magnification image showing a baseball-bat-like structure of fabricated core-shell type solar cell; (b) image showing the variation in radius of CdTe decorated  $\text{TiO}_2$  NR from bottom to top; (c) high-magnification image contrasting the boundary between  $\text{TiO}_2$  and CdTe phases.

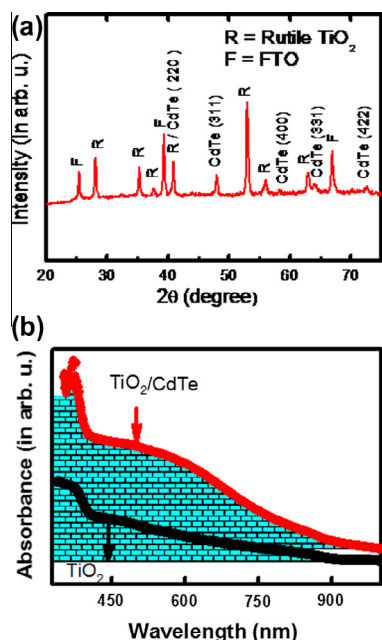


**Figure 3.** (a) XRD pattern recorded for CdTe decorated TiO<sub>2</sub> NR. (b) UV–VIS–NIR absorption spectra obtained for core–shell TiO<sub>2</sub>/CdTe and TiO<sub>2</sub> NR in the 350–1000 nm wavelength range.

the crystal growth rate of CdTe during the sputtering process exceeds the deposition rate, it is expected that there will be sufficient time for the nucleation on the surface of TiO<sub>2</sub> NR to form this type of formation. Furthermore, to investigate the interface region formed between TiO<sub>2</sub> and CdTe, a high-resolution TEM image was recorded and is shown in Figure 2c. The figure shows that not only is the boundary between TiO<sub>2</sub> and CdTe phases differentiable (the brightness contrast between the layers), but the crystal planes of each phase are also clear.

To identify the existing phases in the core–shell structure constructed based on CdTe decorated TiO<sub>2</sub> NR on the FTO pre-coated glass substrate, XRD measurement was carried out. Figure 3a shows the recorded XRD pattern for the fabricated device. The peaks that can be seen emerging from the pattern are associated with FTO, TiO<sub>2</sub> and CdTe, which constitute the components of the designed solar cell [15,17]. The identified phase of TiO<sub>2</sub> NR from the XRD figure belongs to the rutile crystal structure (tetragonal, *P42/MNM*). As for the

CdTe deposited on TiO<sub>2</sub> NR, based on XRD analysis it was identified to be in a cubic system indexed with (111), (220), (311), (400), (331), (422) and (511) planes, as labeled in Figure 3a [17].

The ultraviolet–visible near-infrared (UV–VIS–NIR) absorption spectra of core–shell TiO<sub>2</sub>/CdTe and TiO<sub>2</sub> NR in the 350–1000 nm wavelength range are shown in Figure 3b, taking a FTO pre-coated glass substrate as a reference sample during the measurement. In order to contrast the contribution of the CdTe thin layer, the area under each curve is highlighted. The presence of two onsets observed in the absorption spectrum located at ~885 nm (1.4 eV) and 410 nm (3.02 eV) correspond to the band gaps of CdTe and TiO<sub>2</sub>, respectively, and indicates the absorption contribution of both materials to the absorption process, which enables the broadening of the absorption spectrum including UV, VIS and NIR parts of solar spectrum that can be deduced from the highlighted area under each curve. In other words, a wide range of light spectrum can be absorbed with this type of material-combination-based solar cell, which may promote the fabrication of this type of solar cell, since it is capable of making use of the most abundant part of solar spectrum, covering the energy range between 1.4 eV and 1.6 eV.

The variation in responsivity of the TiO<sub>2</sub>/CdTe core shell device as a function of wavelength in the 300–900 nm range is given in Figure 4a, measured at a reverse bias of 0.5 V at room temperature. The figure shows that photoresponsivity covers photon energies ranging from UV to NIR, consistent with the study of absorption shown in Figure 3b. The spectral variation in photoresponsivity in Figure 4a shows that there are humps located at 600 nm (2.06 eV), 775 nm (1.6 eV) and 854 nm (1.41 eV), among which 854 nm matches the optical band gap of CdTe. As for the others, they may be originating from deep levels in a forbidden energy region related to the defect states formed either in TiO<sub>2</sub> crystal or at the interface formed between TiO<sub>2</sub> and CdTe in core–shell structure, which are contributing to the current under illumination and generate the humps observed in the photocurrent spectrum.

A prototype solar cell based on an n-TiO<sub>2</sub>/p-CdTe core–shell type was fabricated, and its performance was tested under AM 1.5G illumination using an Oriol 1000 W solar cell simulator setup controlled with Newport I–V software. A Cu/Au dot pattern and FTO were assigned as the top and bottom contacts, respectively,

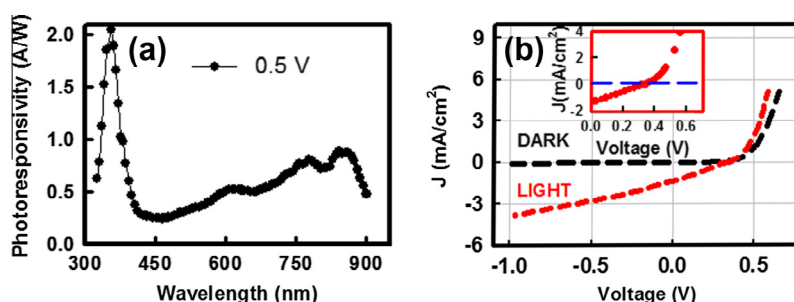


**Figure 4.** Variation in responsivity of TiO<sub>2</sub>/CdTe core–shell device. (b) *J–V* characteristics of n-TiO<sub>2</sub>/CdTe core–shell type solar cell. Inset figure shows the *J–V* characteristic in the 0–0.7 V range.

during the measurement. The current density–voltage ( $J$ – $V$ ) characteristics of the solar cell in the dark and under light illumination are shown in Figure 4b. A rectification of current is observed, verifying the existence of the p–n heterojunction formed between CdTe and TiO<sub>2</sub>. It is clear from the figure that the device exhibits PV behavior that one can deduce from the shift observed in the  $J$ – $V$  curve recorded under illumination with respect to that measured in dark conditions. From the  $J$ – $V$  curve obtained under light illumination, the solar cell parameters such as open circuit voltage ( $V_{oc}$ ), short circuit current density ( $J_{sc}$ ), fill factor ( $FF$ ) and power conversion efficiency ( $\eta$ ) were extracted and found to be 0.34 V, 1.27 mA cm<sup>-2</sup>, 28% and 0.12%, respectively.

It is not possible to compare the solar parameters obtained, since no reported studies have been found elsewhere based on the same structure. However, a core–shell solar cell based on CdTe decorating TiO<sub>2</sub> nanotube arrays was reported by M. Zhang et al. [7]. In that study,  $V_{oc}$  and  $J_{sc}$  were calculated to be 0.23 V and 1.23 mA cm<sup>-2</sup>, respectively with a corresponding power conversion efficiency of 0.10%, which is slightly lower than that obtained with CdTe decorating a TiO<sub>2</sub> NR-based core–shell solar cell. The low performance of the solar cell may stem from the surface states at the TiO<sub>2</sub> and CdTe interface (observed in Figure 4a), which could result in the formation of deep levels as well as shallow levels within the band gap, by which the collection efficiency of photo-generated carriers are significantly reduced. The fabrication of a more efficient solar cell based on core–shell CdTe/TiO<sub>2</sub> NR is possible as long as structural, electrical and optical properties of both core (TiO<sub>2</sub> NR) and shell (CdTe) materials are arranged properly. In other words, there are many issues to be solved in such a solar cell to enhance the power conversion efficiency, including the quality of the deposited thin film (grain sizes, mobility), the morphology of the synthesized TiO<sub>2</sub> NR (length, radius, density and orientation of them), and electrical contacts to CdTe-coated TiO<sub>2</sub> NR. In addition to these, the post-production process, such as CdCl<sub>2</sub> treatment of CdTe thin film, is expected to improve the power conversion efficiency of the solar cell, as it increases grain size in the polycrystalline structure of CdTe, by which the probability of recombination or trapping of charge carriers lowers as a result of the decrease in the number of grain boundaries.

In conclusion, vertically aligned well-oriented TiO<sub>2</sub> NR were synthesized on a FTO pre-coated glass substrate. A CdTe decorated TiO<sub>2</sub> NR-based core–shell type solar cell was fabricated by deposition of a 250-nm-thick CdTe thin film by the RF sputtering tech-

nique. Devices exhibited p–n characteristics in the dark and under light illumination conditions at room temperature. Photoresponsivity measurement revealed that the fabricated device is sensitive to a broad wavelength range from UV to NIR, consistent with study of the absorption spectrum. PV properties were determined under AM 1.5G illumination. For the n-TiO<sub>2</sub>(NR)/p-CdTe(thin film) core–shell type solar cell, the PV behavior was observed, and a 0.12% efficiency was obtained, which suggested that it could be improved by carrying out optimization to increase the quality of the deposited thin film, the morphology of the synthesized TiO<sub>2</sub> NR and contact to CdTe-coated TiO<sub>2</sub> NR.

This work was supported in part by European Union Framework Program 7 Marie Curie IRG Grant 239444 and 249196, COST NanoTP, TUBITAK Grants 109E044, 112M004 and 112E052.

- [1] L. De Marco, M. Manca, R. Giannuzzi, F. Malara, G. Melcarne, G. Ciccarella, I. Zama, R. Cingolani, G. Gigli, *J. Phys. Chem. C* 114 (2010) 4228.
- [2] I.S. Cho, Z.B. Chen, A.J. Forman, D.R. Kim, P.M. Rao, T.F. Jaramillo, X.L. Zheng, *Nano Lett.* 11 (2011) 4978.
- [3] J.B. Chen, C.W. Wang, Y.M. Kang, D.S. Li, W.D. Zhu, F. Zhou, *Appl. Surf. Sci.* 258 (2012) 8279.
- [4] H.W. Lin, Y.H. Chang, C. Chen, *J. Electrochem. Soc.* 159 (2012) K5.
- [5] Z.Y. Fan, D.J. Ruebusch, A.A. Rathore, R. Kapadia, O. Ergen, P.W. Leu, A. Javey, *Nano Res.* 2 (2009) 829.
- [6] B.W. Luo, Y. Deng, Y. Wang, Z.W. Zhang, M. Tan, *J. Alloys Compd.* 517 (2012) 192.
- [7] M.Y. Zhang, Y.N. Wang, E. Moulin, C.J. Chien, P.C. Chang, X.F. Gao, D. Grutzmacher, R. Carius, J.G. Lu, *J. Mater. Chem.* 22 (2012) 25494.
- [8] O.N.B.A. Morales, T. Lopez, S. Sanches, R. Gomez, *J. Mater. Res.* 10 (1995) 2788.
- [9] E. Hosono, S. Fujihara, K. Kakiuchi, H. Imai, *J. Am. Chem. Soc.* 126 (2004) 7790.
- [10] J. Wang, Z.Q. Lin, *J. Phys. Chem. C.* 113 (2009) 4026.
- [11] P.J.R.S.K Pradhan, F. Yang, A. Dozier, *J. Cryst. Growth* 6 (2006) 2009.
- [12] Y.X. Li, M. Guo, M. Zhang, X.D. Wang, *Mater. Res. Bull.* 44 (2009) 1232.
- [13] B. Liu, J.E. Boercker, E.S. Aydil, *Nanotechnology* 19 (2008) 505604.
- [14] B. Liu, E.S. Aydil, *J. Am. Chem. Soc.* 131 (2009) 3985.
- [15] H. Karaagac, L.E. Aygun, M. Parlak, M. Ghaffari, N. Biyikli, A.K. Okyay, *Phys. Status Solidi RRL* 6 (2012) 442.
- [16] M. Ghaffari, M.B. Cosar, H.I. Yavuz, M. Ozenbas, A.K. Okyay, *Electrochim. Acta* 76 (2012) 446.
- [17] K.R. Murali, B. Jayasutha, *Mater. Sci. Semicond. Process* 10 (2007) 36.